Article Identifier
DOI: 10.22032/dbt.58680
URN: urn:nbn:de:gbv:ilm1-2023isc-099:1

60th ILMENAU SCIENTIFIC COLLOQUIUM
Technische Universität Ilmenau, 4 – 8 September 2023
URN: urn:nbn:de:gbv:ilm1-2023isc:1

A novel Point-to-Point length measurement concept based on range-resolved interferometry

Sebastian J. Fischer Calderón, Guido Straube, Thomas Kissinger

Institute of Process Measurement and Sensor Technology, Technische Universität Ilmenau

ABSTRACT

In many fields of research and high-value industry, the estimation of distances and displacements is crucial. Due to their extremely high spatial resolution and flexible application possibilities interferometers are cross-sectorally used in measurement practice. However, classical length measuring interferometers are subject to two residual restrictions. On the one hand, only displacements that are exactly aligned to the interferometer optical axis can be measured. On the other hand, deviating refractive indices in the measuring and reference arm due to different atmospheric conditions represent an accuracy-limiting disturbance. In this paper, a new interferometric concept for length measurement is presented. The concept is based on the range-resolved interferometry technology which enables the simultaneous readout and evaluation of two symmetrical interferometric signals which result from the superposition of two non-collimated spherical wavefronts. This allows a point-to-point measurement between two optical fiber ends and the separation of undesired changes of the optical path length outside the measurement cavity and within the measurement cavity.

Index Terms – Point-to-Point Length Measurement, Range-Resolved Interferometry, Optical Fiber Interferometry

1. INTRODUCTION

Since optical interferometry allows length measurement with sub-nanometer uncertainties [4] commercial interferometers (IFMs) find a wide field of application due to their high-precision performance [2]. Depending on the metrological objective IFMs can be realized in different optical designs [3, 5, 7, 8, 9]**.** Regardless of the specific architecture, the interferometric signal is generated by the superposition of coherent optical wavefronts. Lenght measurement IFMs that are typically used in metrological practice always belong to the group of amplitude splitting IFMs. For this purpose, the primary wave emitted by a laser is split at least once into two partial beams with different optical paths. A reference beam with constant conditions and a spatially fixed wave and a measurement beam with variable conditions and therefore a spatially variable wave. Subsequently, the partial beams are recombined and the phase change respectively the spatial position change can be evaluated. [10] For high-precision length measurements two fundamental requirements emerge from this: first, the refractive index of the medium in the reference arm and in the measuring arm must be nearly identical. If this cannot be guaranteed, a subsequent correction must be made. Due to the high sensitivity of the refractive index to environmental influences, this requires a highly precise and temporally accurate measurement of numerous parameters [1]. Second, to superimpose the partial beams an exact aligned adjustment of the optical axis of the reference beam and the measurement beam is necessary. Consequently, this also requires the exact aligned adjustment of the measurement beam and the target's measurement axis. Not only is the adjustment a time intense and costly process it also reduces the application possibilities of the IFM to displacement measurement in one axis only.

2. METROLOGICAL CONCEPT

This paper presents a novel IFM design that is not subject to these strict limitations and is depicted in Fig. 1. The operation principle is based on range-resolved interferometry (RRI) [6] which allows the isolation and simultaneous phase measurement of multiple constituent IFMs present in a setup based on their optical path differences. This allows the readout of weak interferometric signals even if strong parasitic reflections are present, which is exploited in the proposed concept to isolate the weak signals that result from non-collimated, spherical wave free-space propagation from a point source (single-mode fiber tip). The light source of the setup is an optical frequency-modulated diode laser with an optical wavelength $\lambda = 1550$ nm. Through an x-coupler, the light is split into two in principle symmetric constituted paths. For the distinguishability of the interferometric signal, the optical path length in fiber section 2.1 is significantly longer in the second arm. The circulators (C1, C2) transmit the light to the PC polished fiber end (PC1, PC2) where a part is reflected back into the fiber and a part is emitted into the air gap. A small share of the emitted light is coupled into the opposite fiber end and interferes with the light reflected there. The circulators transmit the interfered wavefront to the detectors (D1, D2) where the signals are demodulated and the phase of the interferences can be evaluated. This allows the calculation of the relative position change of the fiber ends which is proportional to the relative phase change: $\frac{\delta l}{\delta t} \propto \frac{\delta \varphi}{\delta t} \leftrightarrow l' \propto \varphi'$.

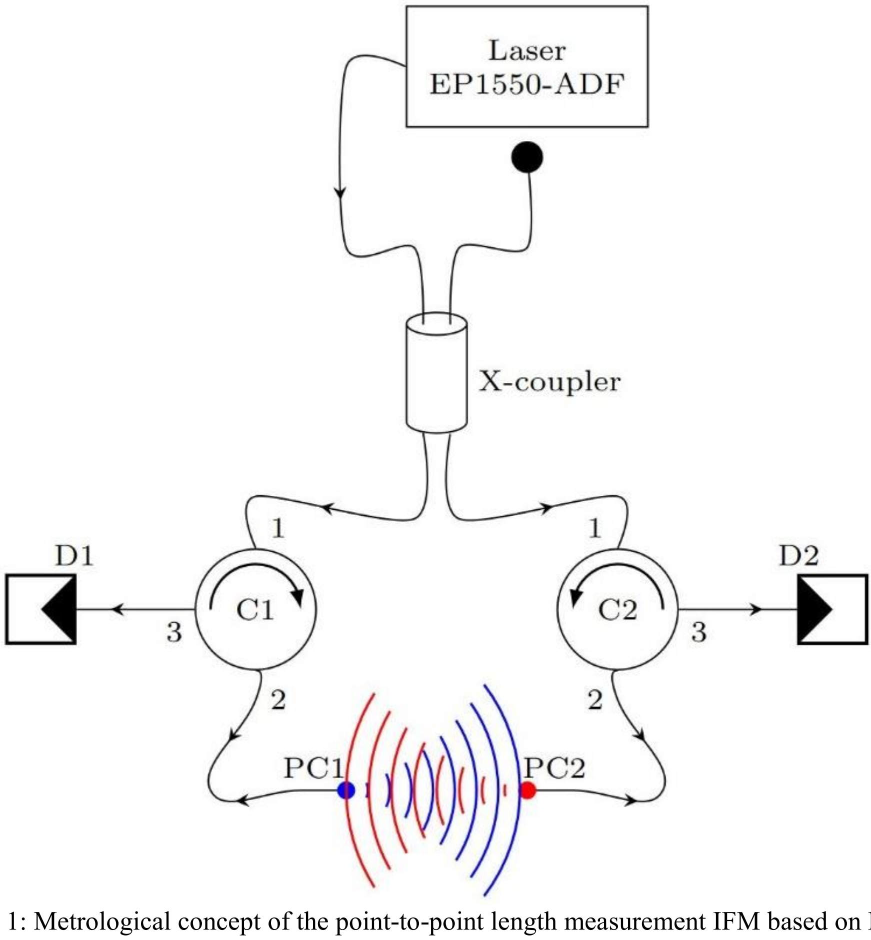

Fig. 1: Metrological concept of the point-to-point length measurement IFM based on RRI.

Due to the symmetrical arrangement and the double readout of the interferometric signals at detectors D1 and D2, the measuring and reference arms of the IFMs are interchanged in each case. For the present arrangement, the considerations are therefore not concentrated in the classical sense on the difference of the optical pathlength between the measuring arm and the reference arm, but on the difference between the optical pathlength within the air gap l'_{in} and outside the air gap l'_{out}. Due to the described setup intrinsic symmetry l'_{in} affects the phase signal in D1 φ_{D1} with a reverse sign to the phase signal in D2 φ_{D2} while l'_{out} affects D1 and D2 with the same sign so that:

$$\varphi'_{\text{D1}} = \varphi'(l'_{\text{in}}) + \varphi'(l'_{\text{out}}) \qquad \varphi'_{\text{D2}} = -\varphi'(l'_{\text{in}}) + \varphi'(l'_{\text{out}}) \tag{1}$$

From a metrological perspective, the interferometric setup shown in this paper differs fundamentally from existing concepts. The RRI technology enables the evaluation of weak interference signals between two non-collimated spherical wavefront. This allows the non-aligned arrangement of the optical axes and can therefore be used for point-to-point distance measurements. Furthermore, the dual sided readout setup allows the separation of the undesired optical path changes outside the air gap from the optical path change to be measured inside the air gap (see Eq.1). This surmounts the restriction of homogeneous conditions of the measuring and reference arm, which is an accuracy-limiting influence in many classical length measuring IFMs.

3. EXPERIMENTAL APPROACH AND RESULTS

The experimental realization of the point-to-point IFM is shown in Fig. *2*. For reasons of clarity, the optical path outside the measurement cavity l_{out} is not shown in its entirety and the measurement cavity l_{in} is primary displayed. In contrast to the schema shown in Fig. 1 the fiber end PC2 was mounted on a manually actuatable linear stage.

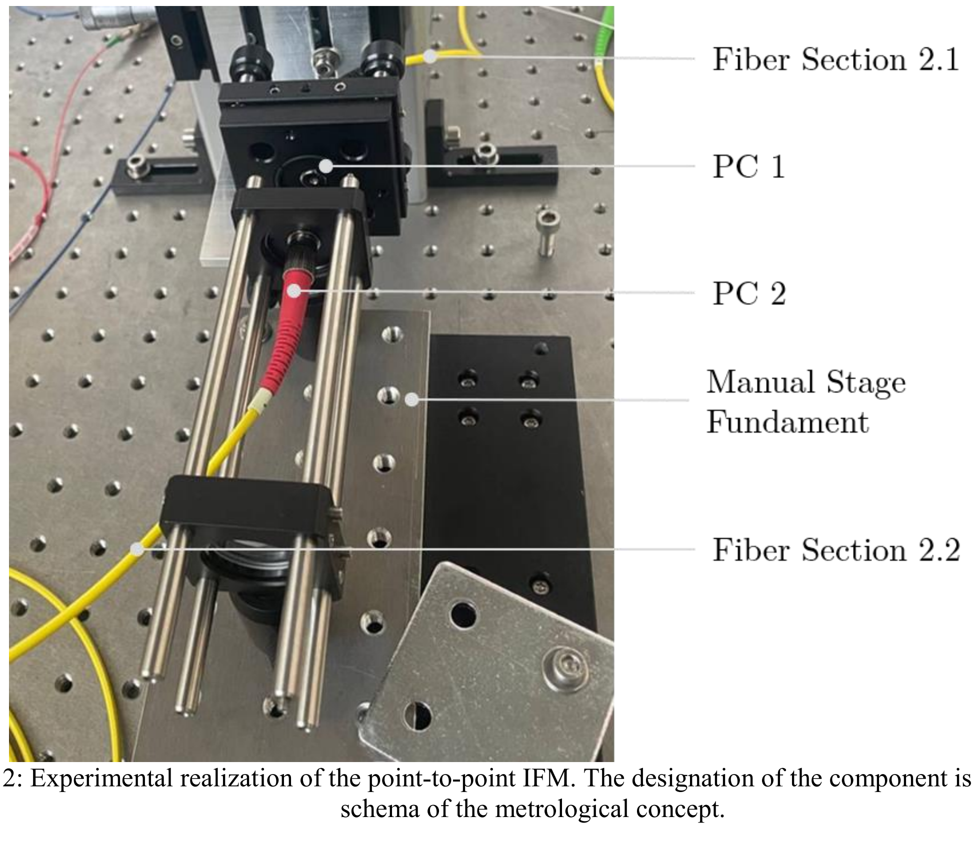

Fig. 2: Experimental realization of the point-to-point IFM. The designation of the component is based on the schema of the metrological concept.

The experimental data depicted in Fig. 3 shows the measured phase signal in D1 and D2 and additionally their difference and summation. During the measurement both, l_{in} and l_{out}, were manipulated simultaneously. The fiber end PC2 which is fixed on the linear stage was manually shifted by Δl_{in}. The motion was initialized the time $t \approx 1{,}3$ s and stopped at $t \approx 3{,}3$ s. The optical path length outside the air gap l_{out} was modified by heating a part of section 1 in the second arm up to 60°C to cause an elongation Δl_{out} during the whole measurement.

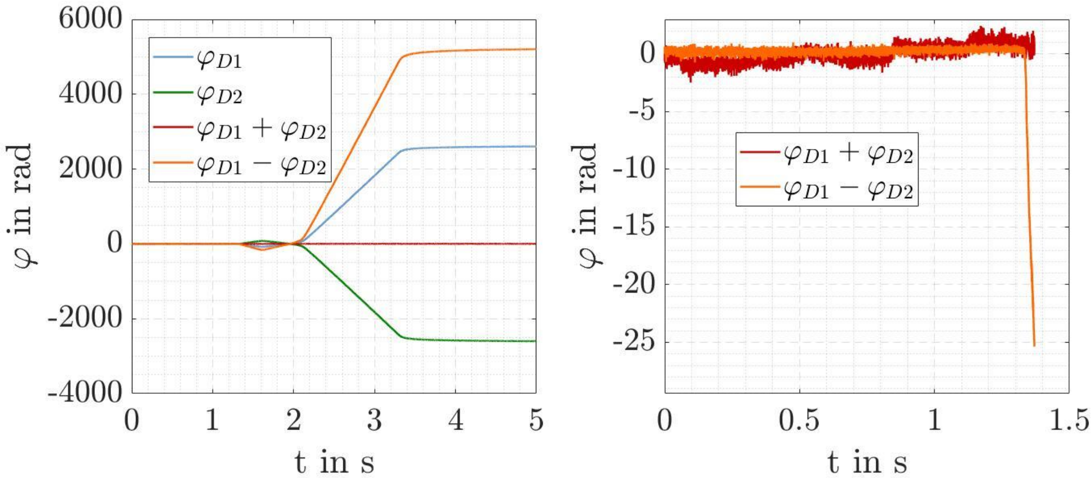

Fig. 3: Illustration of the phase change during a simultaneous manipulation of l_{in} and l_{out}. Left: Phase change in D1, D2 and their difference and sum. Right: Detailed view of the sum and difference signal at the motion initialization within the air gap.

The data in Fig. 3 left shows that the initially flat phase signal in both channels φ_{D1} and φ_{D2} changes correspondingly with the manual actuation of the linear stage between t_{start} and t_{end}. After t_{end} the signal of both phases is nearly flat again. The detailed depiction of the sum and difference of the phase signals at the motion initialization within the air gap l_{in} in Fig. 3 right shows a flat signal with an abrupt change of the difference signal while the sum signal remains nearly constant once the motion is started. The detailed view of the sum signal in Fig. 4 displays a slight drift during the whole measurement with a range of approximately 4 rad.

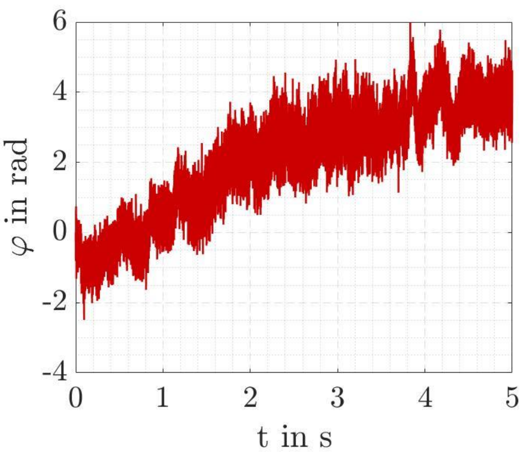

Fig. 4: Detailed view of the sum signal $\varphi_{D1} + \varphi_{D2}$ during the whole measurement.

4. DISCUSSION

The experimental data in Fig. 3 shows accordance to the assumptions postulated in Eq. 1. The implication that the difference of the phases change:

$$\varphi'_{\mathrm{D1}} - \varphi'_{\mathrm{D2}} = 2\varphi'(l'_{\mathrm{in}})$$

is mainly influenced by l'_{in}, shows agreement with the experimental data. This can be seen by the fact that a gradient in the difference signal is only observable when l_{in} is manipulated during the period between t_{start} and t_{end} (see Fig. 3). Also, the phase change of the difference signal between t_{start} and t_{end} of $\Delta\varphi_{diff} = 5150$ rad corresponds with $\Delta l_{\mathrm{in}}$with twofold magnitude. The second implication, that the phase change in the sum signal:

$$\varphi'_{\mathrm{D1}} + \varphi'_{\mathrm{D2}} = 2\varphi'(l'_{\mathrm{out}})$$

is mainly dependent on l'_{out}, can also be seen in the experimental data. The slight drift behavior (see Fig. 4) corresponds with the optical path elongation caused by the warming of l_{out} during the whole measurement. This proves the property of the interferometric concept to separate metrological unwanted changes of the optical path length outside the air gap from the optical path change inside the air gap and the ability to determine them separately. In future research, this property needs to be investigated in more depth by using a broader set of parameters to modify l_{in} and l_{out} and the examination of the influence of the not perfectly symmetrical arrangement of the experimental setup. In addition, the property of length measurement with a non-aligned arrangement of the optical axes must be quantifiably demonstrated. This includes the simulative and experimental investigation of the influence of the relative position of the fiber ends in five degrees of freedom on the metrological performance. On this basis, limits of the relative arrangement of the fibers in space can be determined. This could enable the application of the interferometric concept within the operating principle of multilateration to determine point clouds in 3D space with nanometer accuracy.

REFERENCES

[1] G. Bönsch, E. Potulski, "Measurement of the refractive index of air and comparison with modified Edlén's formulae." Metrologia. IOP Publishing (1998).

[2] A. J. Fleming, "A review of nanometer resolution position sensors: Operation and performance." Sensors and Actuators A: Physical. Elsevier (2013).

[3] P. J. de Groot, "Correlated errors in phase-shifting laser Fizeau interferometry. Applied Optics." Optica Publishing Group (2014).

[4] T. Hausotte, B. Percle, U. Gerhardt, D. Dontsov, E. Manske, G. Jäger, "Interference signal demodulation for nanopositioning and nanomeasuring machines." Measurement Science and Technology. IOP Publishing (2012).

[5] M. R. Islam, M. M. Ali, M.-H. Lai, K.-S. Lim, H. Ahmad, "Chronology of Fabry-Perot interferometer fiber-optic sensors and their applications: a review." Sensors. Multidisciplinary Digital Publishing Institute (2014).

[6] T. Kissinger, T. Charrett, R. P. Tatam, "Range-resolved interferometric signal processing using sinusoidal optical frequency modulation." Optics express. Optical Society of America (2015).

[7] L. Li, L. Xia, Z. Xie, D. Liu, "All-fiber Mach-Zehnder interferometers for sensing applications." Optics express. Optica Publishing Group (2012).

[8] I. Ortlepp; E. Manske, J.-P. Zöllner, I. Rangelow, "Heterodyne standing-wave interferometer/Heterodynes Stehende-Welle-Interferometer." TM - Technisches Messen. Oldenbourg Wissenschaftsverlag (2018).

[9] G. Straube, J. S. Fischer Calderón, I. Ortlepp, R. Füßl, E. Manske, "A Heterodyne Interferometer with Separated Beam Paths for High-Precision Displacement and Angular Measurements." Nanomanufacturing and Metrology (2021).

[10] S. Yang, G. Zhang, "A review of interferometry for geometric measurement." Measurement Science and Technology. IOP Publishing (2018).

CONTACT

Jun.-Prof. Dr. T. Kissinger thomas.kissinger@tu-ilmenau.de